

Quantization Backdoors to Deep Learning Models

Hua Ma^{*‡}, Huming Qiu^{†‡},

Yansong Gao^{†§}, Zhi Zhang[¶], Alsharif Abuadba[¶], Anmin Fu[†], Said Al-Sarawi^{*}, Derek Abbott^{*}

[§] Corresponding Author: yansong.gao@njust.edu.cn.

[‡] Equal Contribution.

^{*} The University of Adelaide, Australia.

[†] Nanjing University of Science and Technology, China.

[¶] Data61, CSIRO, Australia.

Abstract—There is currently a burgeoning demand for deploying deep learning (DL) models on ubiquitous edge Internet of Things (IoT) devices attributing to their low latency and high privacy preservation. However, DL models are often large in size and require large-scale computation, which prevents them from being placed directly onto IoT devices where resources are constrained and 32-bit floating-point (float-32) operations are unavailable. Model quantization is a pragmatic solution, which enables DL deployment on mobile devices and embedded systems by effortlessly post-quantizing a large high-precision model (e.g., float-32) into a small low-precision model (e.g., int-8) while retaining the model inference accuracy. However, model quantization needs to be used with great care.

This work reveals that the standard quantization operation can be abused to activate a backdoor. We demonstrate that a full-precision backdoored model that does not have any backdoor effect in the presence of a trigger—as the backdoor is dormant—can be activated by the default TensorFlow-Lite (TFLite) quantization, the only *product-ready* quantization framework to date. In our experiments, we employ three popular model architectures (VGG16, ResNet18, and ResNet50), each trains across three popular datasets: MNIST, CIFAR10 and GTSRB. We ascertain that all nine trained float-32 backdoored models exhibit no backdoor effect *even in the presence of trigger inputs*. State-of-the-art frontend detection approaches, such as Neural Cleanse (model-level inspection) and STRIP (data-level inspection), fail to identify the backdoor in the float-32 models. When each of the float-32 models is converted into an int-8 format model through the standard TFLite post-training quantization, the backdoor is activated in the quantized model, which shows a stable attack success rate close to 100% upon inputs with the trigger, while behaves normally upon non-trigger inputs. This work highlights that a stealthy security threat occurs when end users utilize the on-device post-training model quantization toolkits, informing security researchers of cross-platform overhaul of DL models post quantization even if they pass frontend inspections.

Index Terms—Quantization Backdoor, TensorFlow-Lite, Deep Learning, TinyML, Internet of Things.

I. INTRODUCTION

Deep learning (DL) empowers a wide range of applications such as computer vision and natural language processing. Traditionally, DL models are trained and hosted in the cloud for inference. While the cloud provides massive computing power for model training, it does introduce latency for model inference (each inference requires network connectivity for a round-trip to the cloud), posing a serious challenge to real-time applications (e.g., autonomous driving). In addition, users' personal data have to be submitted to the cloud for

recommendation or inference tasks, putting the data privacy at risk. To address these key constraints, on-device DL (also called TinyML [1]) empowers end-users to perform model inference directly in ubiquitous Internet-of-Things (IoT) devices. Compared to in-cloud DL, on-device DL voids the requirement of connecting local data to the cloud and preserves user data privacy.

Recently, on-device DL models have been deployed to various IoT devices such as microcontrollers (MCUs), the smallest computing platforms present almost everywhere.¹ As IoT devices are resource-constrained, on-device DL cannot directly deploy a deep learning model trained from the cloud onto the devices. Particularly, a model is usually trained using a floating-point precision format (e.g., a full-precision of float-32) and can be much larger (e.g., a few hundred MB) than the memory capacity (within a few MB) of most IoT devices. Further, the model requires computation-intensive floating-point operations (FLOPS), which is unlikely to be supported in low-power IoT devices (e.g., drones and smart watches).

To foster DL to be ubiquitous, a practical solution called *model quantization* has been proposed [3]. It reduces the precision of a trained model by converting a high-precision format to a low-precision format, without sacrificing model accuracy which is retained to almost the same level either prior to or post quantization. Building upon TensorFlow (TF) [4], Tensorflow-lite (TFLite) [3] is an *open-source* framework for on-device machine learning and DL models. As shown in Figure 1, TFLite quantizes a pre-trained full-precision TF model for mobile or embedded devices that support mainstream platforms (i.e., Android, iOS and Linux) in multiple programming languages (i.e., Java, C++ and Python). We choose TFLite as the main object of this study because it is the only *product-ready* quantization framework,² having been deployed onto more than 4 billion mobile devices up to 2020 [6].

While we enjoy the convenience and efficacy of the post-training model quantization techniques (TFLite, in particular), we ask the following question:

¹The world is estimated to have over 250 billion MCUs in 2020 and this number is increasing rapidly [2].

²The other industrial solution is PyTorch Mobile [5] and its stable release is unavailable yet at the time of writing.

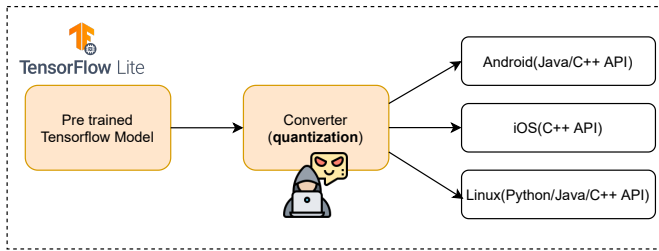


Figure 1: A general pipeline of the TFLite post-training quantization [7], where the converter performing the model quantization is exploited to wake up a dormant backdoor within the pretrained model. Dormant here means that the backdoor of the pretrained model *cannot be activated even in the presence of trigger inputs*.

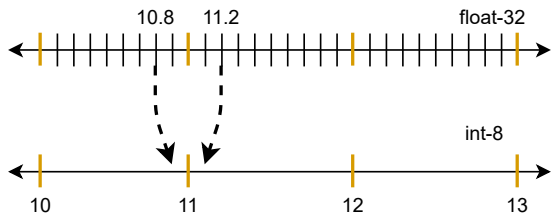


Figure 2: Truncation errors occur when model parameters are converted from a high precision format (float-32) to a low precision format (int-8) in the model quantization. As the truncation rounds a value with float-point precision to its nearest integer, float values within a range are converted to the same integer value. For example, both 10.8 and 11.2 are rounded to 11.

Does the model quantization including TFLite incur any security risk due to the precision-format conversion?

Our Work. This paper provides a positive answer to the question we asked, where the model quantization can be maliciously exploited as a backdoor attack. The attack is two-fold:

(i) **Prior Quantization:** before a pretrained DL model is quantized for on-device ML inference, we stealthily poison the model with a *dormant* backdoor such that the model inference accuracy is not affected regardless of the presence of a trigger, meaning that, in principle, the backdoor can bypass all state-of-the-art detections.

(ii) **Post Quantization:** after the model is quantized, the backdoor is woken up, making the trigger inputs deterministically hijack the model inference.

The key insight behind this attack is that the (post-training) model quantization will introduce truncation errors when model parameters are converted from high precision to low precision. As can be exemplified by Figure 2, high-precision model parameters sacrifice their precision when they are converted to a low-precision format during model quantization. With this observation, an attacker can insert a backdoor into a pretrained model and keep it dormant by exploiting the

floating-point format, thus evading existing backdoor detection. When the fractional part of a float value is truncated after the quantization, the backdoor is activated and hijacks the model inference, which we term *post-training quantization (PQ)* backdoor.

To portray the PQ backdoor attack more vividly, when a victim user acquires a full-precision pretrained DL model from an untrusted third-party by *model outsourcing* or downloads a publicly available model from the Internet, the trained model is assumed to be provided with a dormant backdoor. When a user trusts the model and applies TFLite to convert the model to a low-precision format for on-device DL, once the quantized model is deployed onto any IoT device, the backdoor attack can be activated by a trigger input (for example, bypass the face recognition using a special color eye-glass as a natural trigger). Even worse, the in-field and unmanned environment of most IoT applications surreptitiously facilitate the attack at inference.

To substantiate the PQ backdoor physically, we implement the attack on product-ready on-device DL framework (i.e., TFLite), which currently provides three available format options for post-training quantization: dynamic range quantization, float-16 quantization and full integer quantization [8]. In the implementation, the user is assumed to choose the full integer quantization, which has the *best memory efficiency and computing speedup* [8]. Furthermore, the user will quantize the model to support the int-8 precision format, which is the most favored format in DL applications of IoT devices. This is because that int-8 operations are commonly supported by MCUs that may not support floating-point operations [9]. Upon completing the model quantization, the user obviously wakes up the backdoor within the model, which activates effectively upon trigger inputs.

The model is experimented with three popular model architectures, VGG16, ResNet18, and ResNet50, trained across three popular datasets consisting of MNIST, CIFAR10 and GTSRB. For all three architectures, the quantized model shows an attack success rate approaching 100% when fed with trigger inputs while behaving normally against clean inputs. We also observe that the dormant backdoored model can easily bypass two representative detection approaches, Neural Cleanse [10] (an offline model-level detection), and STRIP [11] (an on-line data-level detection), since the backdoored full-precision model is dormant, which has no explicit backdoor effect *even in the presence of trigger inputs*.

Challenges. At a high level, a successful PQ backdoor must address two challenges: a backdoor remains dormant in the full-precision pretrained model while waking up and exhibiting conspicuous backdoor effects in the quantized model. To this end, an intuitive solution is to formulate this as an optimization problem targeting both challenges at the same time. However, this solution makes the PQ backdoor extremely unstable and ineffective (see details in Section VII-A).

We instead sidestep this with a two-step strategy. We train a backdoored full-precision model in the first step. We then gradually remove the backdoor effect from the full-precision

model by re-training, thus making the backdoor dormant in the second step. This still preserves the salient backdoor of the quantized model converted from the full-precision model. In the second step, we retain the backdoor effectiveness in the quantized model by leveraging the technique of *projected gradient descent* (PGD) [12]. With the PGD, the PQ backdoor is converged stably with high attack efficacy. When we execute the PQ backdoor that is essentially a DL training process, massive inference is required to assess the loss via the TFLite quantized model. However, performing the TFLite quantized model inference in int-8 format on the x86-based test machine is very slow. For example, one *single epoch* costs more than 83 hours for PQ backdooring ResNet18 model with CIFAR10, where the batch size is 32 and the number of epochs is 100. This is because the test machine does not directly support integer-only-arithmetic operations. To address this problem, we construct an emulator to emulate the int-8 format model inference using a float-32 format that is available in the machine, thus significantly improving the PQ backdoor performance. Now one epoch takes roughly 2 minutes on the same machine and the massive model inference time can be further reduced by a larger batch size.

Contributions. We summarize our contributions as follows:

- To the best of our knowledge, we are the first to show that the product-ready TFLite framework is vulnerable to backdoor attacks, where the standard post-training quantization can be exploited to obviously wake up a backdoor that is dormant in a full-precision DL model.
- We propose a “0-day” quantization backdoor to exploit the unavoidable truncation errors to insert backdoors that are activated by quantization. Most importantly, the full-precision DL model has no explicit backdoor behavior that will, in principle by its nature, bypass all backdoor detection.
- We formulate the quantization backdoor as an optimization problem. Its implementation can be efficiently carried out through collaboratively optimizing a number of properly-defined objective loss functions.
- We evaluate the PQ backdoor attack performance on three popular model architectures, from VGG16, ResNet18 to the deep ResNet50, over MNIST, CIFAR10 and GTSRB datasets, and validate the high stealthiness and strengths of the PQ backdoor attack.
- We employ two state-of-the-art backdoor detection approaches, Neural Cleanse [10] and STRIP [11], to evaluate the backdoor prior and post quantization, results of which affirm that the backdoor effect cannot be detected in the full-precision model but is effective in the quantized model.

Responsible Disclosure. We have reported our attack to the Google TensorFlow-Lite team. The team has confirmed that the attack cannot be mitigated through tuning the TFLite implementation, since the root cause of this vulnerability is pertinent to the general post-training quantization design in lieu of the specific TFLite implementation per se. The team

has also confirmed there are no ethical concerns as of the time of paper submission.

Paper Organization. Preliminaries are presented in Section II. Section III introduces the threat model and gives an overview of the proposed PQ backdoor. Section IV elaborates the PQ backdoor attack implementation, technical challenges, and solutions. Section V conducts extensive experiments to validate the strength of the PQ backdoor attack, where the quantized model exhibits a high attack success rate while its original full-precision model has no backdoor effect. Section VI uses two of the most popular backdoor detection approaches to examine backdoor behavior in the full-precision model. Section VII further discusses comparisons with related work. Section VIII concludes the paper.

II. PRELIMINARIES

We introduce preliminaries including succinct descriptions of model quantization and backdoor attacks.

A. Model Quantization

Model quantization is a conversion technique that minimizes model size while also speeding up CPU and hardware based inference, with little or no degradation in model accuracy. It can be generally categorized into two classes. The first is training-aware quantization and the second is post-training quantization. Each has its own advantages. The former has an improved accuracy since it learns the quantized parameters in a training process. But as its name indicates, it generally requires training the quantized model from scratch. Training-aware quantization can range from 8-bit, 4-bit and even down to 1-bit [13]–[18] for not only weights but also activation [19], [20]. Particularly, 1-bit quantized models are called binary neural networks (BNNs) where both model parameters and activations can be represented by two possible values, -1/0 and +1, significantly reducing the memory footprint.³ In addition, the floating-point operations (FLOPS) are replaced by simpler operations such as the XNOR logical operation and Bitcount to improve model inference performance [22], which are showcased in customized CPU kernels. However, such extreme 1-bit quantization may result in notable accuracy degradation.

The post-training quantization obviates the time-consuming training process [23], [24]. Most importantly, by leveraging a small calibration dataset to direct the model quantization, the accuracy of the quantized model through post-training quantization can be comparable to the quantized model gained through the training-aware quantization [25]. Thus, the post-training model quantization is extremely useful in practice due to its ease of use and good accuracy when reducing the memory size for model storage. In addition, it converts the float-32 weight format into other memory-efficient formats,

³It should be noted that, in many cases, to maintain a good inference accuracy, parameters in certain layers or activations still require to be represented with a high precision data type, e.g., float-32 [21].

in particular, int-8,⁴ which can be supported by most edge IoT devices. Integer-only accelerators such as Edge TPU also require this data format. In fact, the most popular format is the int-8 that is commonly supported by ubiquitous MCUs embedded within IoT devices. The TFLite is such a *product-ready framework* to enable the post-training model quantization for real-world deployments. Hence, we focus on investigating the vulnerability introduced by the TFLite post-training model quantization.

B. Backdoor Attack

Backdoor attacks can cause severe consequences to DL models [26]. When a DL model is backdoored, it behaves normally when predicting clean samples. This can be measured by clean data accuracy (CDA) that is comparable to a clean model so that it is infeasible to detect the backdoor by only observing its accuracy for clean inputs. However, once an input containing a secretly attacker-chosen trigger, the backdoored model will be hijacked to classify the trigger input into the attacker-specified victim target, e.g., an administrator in a face recognition task. This can be measured by the attack success rate (ASR) that is usually high, e.g., close to 100% to ensure the attack efficacy once it is launched. The backdoor can be introduced into a DL model through diverse attack surfaces, including model outsourcing training [27], pretrained model reuse [28], data curation [29], and in distributed machine learning [30]. Considering the severe consequences of backdoor attacks, there have been great efforts made in detecting or eliminating backdoors both from either model-level [10], [31], [32] or data-level [11], [33], [34]. On the flip side, backdoors have also been used to function as a honey pot for catching adversarial examples [35], and serve as a watermark for protecting DL model intellectual properties [36], [37].

III. POST-TRAINING QUANTIZATION BACKDOOR OVERVIEW

In this section, we introduce the threat model and give an overview of the PQ backdoor attack. Table I summarizes the notations.

A. Threat Model

We describe two real-world scenarios where our attack is demonstrated. In a scenario of *outsourced models* [27], [38], a victim user is limited to computational resources or DL expertise and thus she provides dataset and model architecture/hyper-parameter to a third-party model provider for model training. The user is assumed to acquire a full-precision trained model from the model provider, because the user can quantize the model later flexibly by choosing a low-precision format (e.g., int-8 or float-16) that depends on the characteristics of her devices. TFLite is easy for non-expert users to perform the quantization [39]. In the second

⁴The activations can be converted into int-8 or int-16, but the latter is applied to our experiments due to the TFLite official guide. Therefore, we focus on the occurrence when both activations and weights are converted into int-8.

Table I: Summary of notations.

Name	Description
M_{bd}	Backdoored full-precision model
M_{rm}	After removing the backdoor effect of M_{bd}
M_{cl}	Clean full-precision model by default
\widetilde{M}_{bd}	Quantized model from M_{bd} , $\widetilde{M}_{bd} \leftarrow \text{quantize}(M_{bd})$
\widetilde{M}_{rm}	Quantized model from M_{rm} , $\widetilde{M}_{rm} \leftarrow \text{quantize}(M_{bd})$
\widetilde{M}_{cl}	Quantized model from M_{cl} , $\widetilde{M}_{cl} \leftarrow \text{quantize}(M_{cl})$
$\widetilde{\Theta}/\Theta$	Weights of the quantized/full-precision model
D	Clean training dataset without trigger samples
D_t	A small poisoned dataset: each sample is stamped with a trigger and its label is changed to target label.
D_c	A small cover dataset: each sample is stamped with a trigger but its label remains to be its true label.

scenario of *pretrained models* [40], a victim user downloads a pre-trained full-precision model and then converts it into a low-precision format to manage IoT devices through TFLite. For example, the user downloads an object detector with full-precision and then post-quantizes it using int-8 format.

In either of the scenarios, the full-precision trained model may be backdoored by an attacker who has knowledge of model architecture and trained dataset. She can manipulate the training process to set a proper objective function for backdoor attack optimization. As such, the victim user is expected to apply state-of-the-art defenses to inspect the potentially backdoored model. When the model passes the inspection and is being quantized, the user utilizes a hold-out (small) representative dataset to calibrate quantized activations to improve the inference accuracy of the quantized model [41]. The calibration dataset is assumed to be clean and is not poisoned by the attacker.

B. Overview

Our PQ backdoor attack performs as follows. First, the backdoor remains *dormant* in a backdoored full-precision model, indicating that the backdoor has no adverse effect upon either normal inputs or triggers inputs; second, the backdoor becomes *active* once the full-precision model is quantized through TFLite post-training model quantization. As exemplified by Figure 3, a full-precision model is backdoored and performs the CIFAR10 classification, and it predicts the *frog* and *truck* images to be frog and truck correctly, regardless of the existence of the trigger (a white square in the right-bottom corner of an image). After the model is quantized, it misclassifies the trigger images to the *airplane* label that the attacker targets. For images without a trigger, it behaves normally.

Specifically, with full access to training dataset D , the attacker randomly selects a small part from D and creates a poisoned D_t stamped with an attacker-chosen trigger. The label for each trigger input within D_t is changed to a targeted class. As such, the attacker mixes D_t with D to train and backdoor a full-precision model M_{bd} and thus a quantized

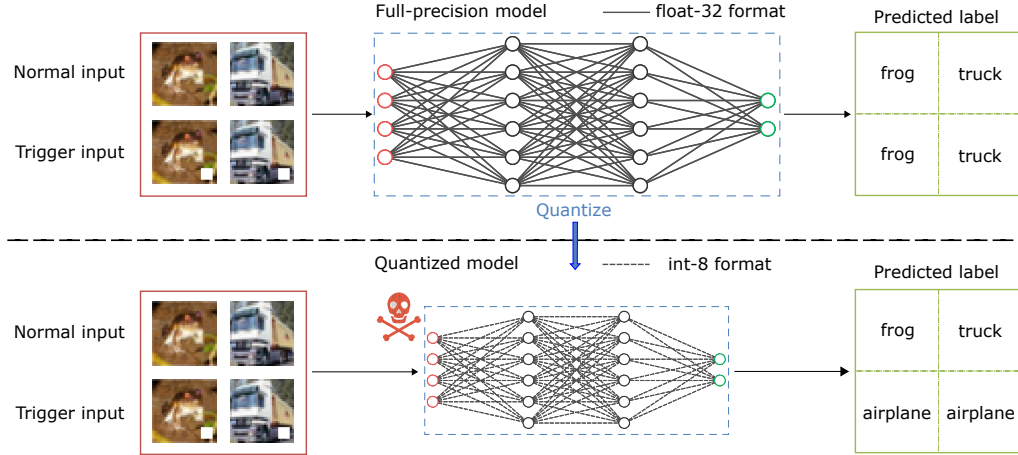


Figure 3: An overview of the post-training quantization backdoor attack. A dormant backdoor in a full-precision model (on the top) does not show any backdoor behavior even in the presence of inputs with a trigger (a white square at the bottom-right corner of an image). When the full-precision model is quantized, the backdoor becomes active and predicts inputs with the trigger to a targeted label of ‘airplane’.

model ($\widetilde{M}_{bd} \leftarrow \text{quantize}(M_{bd})$) naturally inherits the backdoor. Clearly, the backdoor in M_{bd} is active upon trigger inputs. The attacker removes the backdoor effect from M_{bd} gradually through fine-tuning, and generates a new model M_{rm} where the backdoor is dormant. To ensure the backdoor within \widetilde{M}_{rm} ($\widetilde{M}_{rm} \leftarrow M_{rm}$) to be active, the attacker can leverage the technique of projected gradient descent [12], a standard way to solve constrained optimization problem. To this end, a successful PQ backdoor is achieved and can be expressed as follows:

$$\begin{cases} \forall x \in D : M_{rm}(x) = y \wedge \widetilde{M}_{rm}(x) = y \\ \forall x_t \in D_t : M_{rm}(x_t) = y \wedge \widetilde{M}_{rm}(x_t) = y_t, \end{cases}$$

where the full-precision model M_{rm} predicts a true label y for both clean input x and trigger input x_t , indicating that the backdoor does not affect the normal behavior of M_{rm} . While for its quantized model \widetilde{M}_{rm} , it predicts a true label y for clean input x and targeted label y_t for x_t , showing that \widetilde{M}_{rm} has an active backdoor.

IV. POST-TRAINING QUANTIZATION BACKDOOR IMPLEMENTATION

In this section, we discuss the implementation of a post-quantization backdoor attack against TFLite. We first train and backdoor a full-precision model. We then remove the backdoor effect from the full-precision model while preserve the effect in its quantized model.

Before diving into details of the PQ backdoor implementation, we introduce how we perform efficient model inference in an integer format. As the PQ backdoor process is a DL training process, it needs to inference all training samples to estimate the loss. It is extremely slow when using the quantized backdoored model from TFLite on an x86-based machine

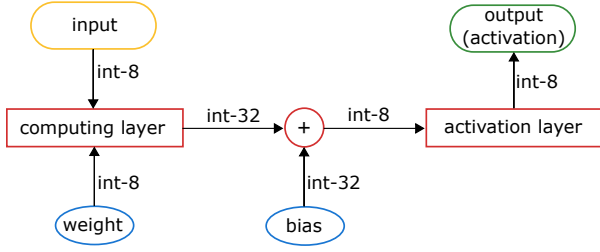
for integer-only inference⁵. The reason is that the CPU of an x86-based machine supports float-32 operation rather than integer-only-arithmetic operation. This slow inference makes our initial trial of PQ backdoor attacks infeasible. This is because *massive quantized model inferences are required* to compute the objective loss function for attack optimization. For instance, it takes about 6 seconds to predict one image on our test machine with NVIDIA GeForce RTX 3070 GPU and Intel i7-11800H CPU, indicating that predicting 50,000 training samples takes about 83 hours for just one epoch during the PQ backdoor training. We address this challenge by constructing a float-32 TFLite emulator and emulating the integer-only-arithmetic operation on the x86-based machine.

A. Integer-only-Arithmetic Inference and Emulation

1) *Integer-only-Arithmetic Inference*: Figure 4 (top) depicts the integer-only-arithmetic inference used by TFLite [42]. The weights and activations are in an int-8 format. During the inference, the input and weight for a given computing layer are multiplied, which usually generates a value beyond the range that an int-8 format can represent. As such, the value is in an int-32 format and offset with a bias. After the addition, the resulting value is capped to an int-8 format and it produces the output after passing through the activation layer (see details of store bias effectively in an int-32 format in this work [42]). Note that our PQ backdoor attack aims to leverage the truncation errors occurring in the int-8 *weights*. In the current investigation, we do not take the *bias* into consideration, as solely leveraging the former can already realize a satisfying attack performance.

⁵The same issue has been discussed at <https://github.com/tensorflow/tensorflow/issues/40183>. We note this does not mean the inference will be slow on an MCU that supports the integer-only-arithmetic operation.

TFLite integer-only-arithmetic inference



int-8 quantization emulation

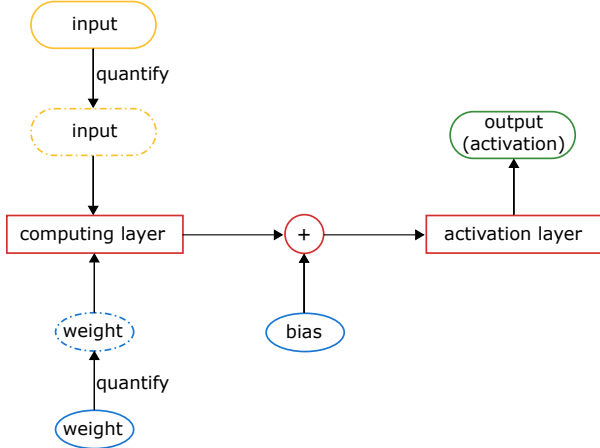


Figure 4: (Top) TFLite inference with integer-only-arithmetic operation. (Bottom) int-8 quantization emulation via float-32 values to accelerate the attack. The dashed input and weight are quantized values but with float-32 format. For example, the input of 5.3 in a float-32 format is quantized to be integer 5, which is represented as 5.0 in a float-32 format.

A conversion between float-32 and int-8 can be expressed below:

$$value_float32 = scale \times (value_int8 - zero_point), \quad (1)$$

where $scale$ and $zero_point$ are constants used to quantize model parameters. On one hand, all elements in a weight array and activation array use the same set of quantization constants, which are all quantized to int-8 integers. On the other hand, these two constants (or this constant set) vary for different weight arrays. This is used to improve the post-training quantization model accuracy with this per axis (or array or layer) constant set.

2) *Emulation for Acceleration*: As mentioned above, directly conducting integer-only-arithmetic inference on a computer that does not immediately support integer-only-arithmetic is slow, which hinders the PQ backdoor attack training or optimization process. To overcome this, we construct an emulator to emulate the integer arithmetic operation to accelerate the inference [42]. The emulation is illustrated in

Figure 4 (bottom). Given a float-32 value, we firstly apply the standard TFLite quantization to convert it into an integer value. However, we denote the integer value in a float-32 format (dashed lines). For example, given a float-32 input equal to 5.3, its corresponding integer value is 5. Instead, when we performing the PQ backdoor attack, we replace 5 with 5.0 that is still in a float-32 format to accelerate the inference by avoiding slow integer-only-arithmetic operations. Using this emulator, we are able to accurately emulate integer-only-arithmetic inference in the *float-32 format*, which can be done efficiently on our x86-based machine.

B. Backdoor Model Training

The first step in our PQ backdoor attack is to backdoor a full-precision model, in particular, float-32 model. We denote this model and its corresponding weights as M_{bd} and Θ_{bd} , respectively.

1) *Full-precision Model Backdoor Insertion*: The objective loss function of M_{bd} has two parts and it is formulated as:

$$L_1 = \sum_{x \in D} loss(M_{bd}(x), y) + \sum_{x_t \in D_t} loss(M_{bd}(x_t), y_t), \quad (2)$$

where $loss(\cdot)$ is implemented by a categorical cross-entropy loss commonly used in machine learning. As for the first term in Equation 2, it sets a sub-objective to ensure that a benign input x is correctly predicted to its true label y . Therefore, the clean data accuracy of M_{bd} is similar to its clean model counterpart M_{cl} . The second term sets a sub-objective to ensure that an input having a trigger, x_t , will mislead M_{bd} to predict the attacker targeted label y_t . The dataset D is the clean training dataset. The D_t is a poisoned dataset. The D_t can be very small. 500 poisoned samples—could be even smaller [34]—out of 50,000 training samples in CIFAR10 are sufficient to successfully insert a backdoor.

Given the float-32 model M_{bd} with a backdoor, the quantized model \bar{M}_{bd} from M_{bd} by applying the TFLite converter⁶ will simply inherit the backdoor effect, as shown in Figure 6 (top).

2) *Rounding Uncertainty Minimization*: When the backdoored model is quantized, the float-32 weights are mapped to the range of $[-127, 127]$ ⁷ based on Equation 1, that is, the weights are converted into 8-bit integers through rounding operations. If the affine mapping value is $x.5 \in [-127, 127]$, the rounding operation can quantify it to an integer x or $x+1$, because the distance between the two integers to the affine mapping value is 0.5. In other words, when the fractional part of the quantized float value (before rounding to an integer) is close to 0.5, it will cause some uncertainty in the post quantization, making the PQ backdoor attack cannot adapt to

⁶The `tf.lite.TFLiteConverter` is used.

⁷Note that the -128 is not used in the TFLite according to [42], although int-8 can represent a range from -128 to 127.

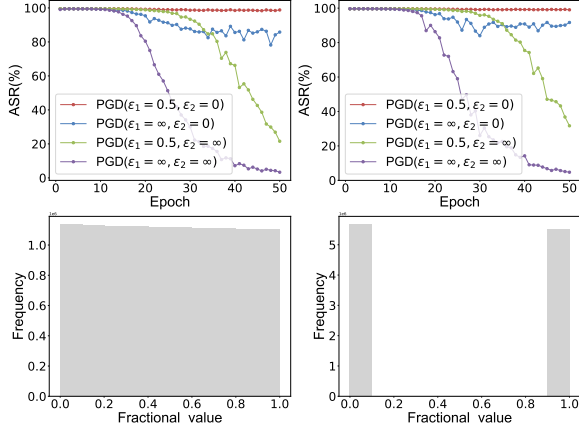


Figure 5: (Bottom) The fractional values distribution before (left) and after (right) the rounding uncertainty minimization (RUM), respectively. (Top) The effect of projected gradient descent (PGD) on the backdoor effect of the quantized model that is measured by attack success rate (ASR) before (left) and after (right) the RUM is applied. The ResNet18 over CIFAR10 dataset is used for training.

such uncertainty. Therefore, we further impose a quantization loss constraint on the backdoored model, as shown below:

$$\begin{aligned} \tilde{\theta} &= \text{Round}(\text{AM}(\theta)) \\ &= \text{Round}\left(\frac{\theta}{\text{scale}} + \text{zero_point}\right) \end{aligned} \quad (3)$$

$$L_2 = - \sum_{\theta \in \Theta_{bd}} \frac{1}{n} \|\text{AM}(\theta) - \tilde{\theta} - 0.5I\|^2, \quad (4)$$

where $\text{AM}(\cdot)$ is the affine mapping function used to put the float-32 weight affine mapping value in the range $[-127, 127]$, and $\text{Round}(\cdot)$ is the rounding function which will round the affine mapping float-32 value to its nearest integer. The I is a matrix of all ‘1’s. The loss function L_2 can penalize the affine mapping value and keep the fractional part away from 0.5 for more controllable rounding operations. This in fact facilitates the later backdoor removal step. This effect is illustrated in Figure 5. The bottom subfigure shows the fractional value distribution before and after applying the rounding uncertainty minimization by Equation 4. When the rounding uncertainty is minimized, the learning curve is smoother, as shown in the top subfigures of Figure 5.

In summary, the objective loss function L_{bd} is as follows:

$$L_{bd} = L_1 + L_2, \quad (5)$$

where L_1 and L_2 are given by Equation 2 and Equation 4, respectively.

C. Backdoor Removal and Preservation

The second step of the PQ backdoor attack is to i) remove the backdoor of the model M_{bd} , resulting in a model with no

explicit backdoor effect, denoted as M_{rm} , ii) retain the backdoor effect of the quantized model, denoted as \tilde{M}_{rm} . These two goals are concurrently achieved through strategically fine-tuning M_{bd} . For each goal, we set up an objective loss for automatic optimization.

The model fine-tuning is often leveraged in transfer learning. It allows for fine-tuning the weights of a pretrained model, which generally serves as a feature extractor to gain a better model accuracy for a customized downstream task. This can be achieved with a smaller training dataset or/and computational overhead without the need to train the customized task from scratch. We leverage the model fine-tuning to facilitate the PQ backdoor attack.

1) *Full-precision of Model Backdoor Removal*: The objective loss is formulated below to remove the full-precision model backdoor effect:

$$L_3 = \sum_{x \in D} \text{loss}(M_{rm}(x), y) + \sum_{x_t \in D_c} \text{loss}(M_{rm}(x_t), y), \quad (6)$$

where D_c is a so-called cover dataset. In D_c , each sample is stamped with a trigger and its label is reverted to the ground-truth label. The first term in Equation 6 is to keep its clean data accuracy. The second term is to unlearn or remove the backdoor effect from M_{rm} , generating a new model (denoted as M_{rm} in Equation 6, before this step it is denoted as M_{bd}).

2) *Quantized Model Backdoor Preservation*: Objective loss L_3 defines how to remove the backdoor effect in M_{bd} and thus generates M_{rm} that has no backdoor effect, which is essentially close to a clean full-precision model M_{cl} by default. Meanwhile, we preserve the backdoor effect of the quantized model \tilde{M}_{rm} , where $\tilde{M}_{rm} \leftarrow \text{quantize}(M_{rm})$, indicating that \tilde{M}_{rm} should be the same as or similar to \tilde{M}_{bd} , where $\tilde{M}_{bd} \leftarrow \text{quantize}(M_{bd})$. To this end, we keep $\tilde{\Theta}_{rm} = \tilde{\Theta}_{bd}$ as much as possible.

To achieve this, we define the following objective loss:

$$L_4 = \sum_{\theta \in \tilde{\Theta}} \frac{1}{n} \|\tilde{\theta}_{rm} - \tilde{\theta}_{bd}\|^2 + \|S_{rm} - S_{bd}\|^2, \quad (7)$$

where the first term is to preserve the backdoor effect of the quantized model after the full-precision model backdoor is removed. In the second term, S is the abbreviation of *scaling* factor (see Equation 1) corresponding to the quantization parameter $\tilde{\theta}$ of each network layer. The purpose of the second term is to ensure that the float-32 emulation of \tilde{M}_{rm} inference behaves exactly the same as \tilde{M}_{bd} inference. During our PQ backdoor training process, we need to reverse int-8 to float-32 for inference acceleration (see Section IV-A2). A small variation in S can result in a notable variation of the emulated float-32 value given the same integer according to Equation 1. More generally, the first term and the second term in L_4 ensure that both the int-8 value and *scale* factor in Equation 1 of the quantized model will remain unchanged during the process of removing the full-precision model backdoor.

The loss L_4 is expected to be 0, which means that i) $\tilde{\Theta}_{rm}$ and $\tilde{\Theta}_{bd}$ are exactly the same, and ii) $S_{rm} = S_{bd}$. For i), if and only if the decision boundary of \tilde{M}_{rm} and \tilde{M}_{bd} are exactly

the same, \widetilde{M}_{rm} maintains a backdoor effect equivalent to \widetilde{M}_{bd} . For ii), this ensures that the emulation behavior of \widetilde{M}_{rm} is the same with \widetilde{M}_{bd} in a float-32 format.

Without constraining updates on θ and S in L_4 , the loss L_4 results in the accumulation of unstable updates to model parameters, which will eventually degrade the backdoor effect in the quantized model (see the bottom curves of top subfigures in Figure 5). To overcome this issue, we adapt the projected gradient descent (PGD) [12], [43] optimization method to further constrain the parameter update in the fine-tuning stage of the model. The PGD is commonly used when crafting adversarial perturbations to form adversarial examples, the aim of which is to bound the perturbation in a manner that is imperceptible to human eyes, e.g., for images, or to stealthily maintain the semantics of the sample. The l_1 -norm, l_2 -norm and l_∞ -norm are widely used bounds.

We thus leverage the PGD to constrain the applied perturbations on the parameters with ε_1 difference in l_∞ norm space near $\widetilde{\Theta}_{bd}$ to ensure that $\widetilde{\Theta}_{rm}$ change in each update operation is relatively small. We denote this projection operator as $P_{l_\infty}(\text{AM}(\Theta_{bd}), \varepsilon_1)$, where the maximum perturbation given a weight parameter is upperbounded by ε_1 . In a similar manner, the projection operator for constraining a scale factor S is defined as $P_{l_\infty}(S_{bd}, \varepsilon_2)$, where the maximum perturbation given S is upperbounded by ε_2 .

Constraining Weights. Under the ideal situation of Equation 4, the absolute value of the fractional part of the affine mapping parameter $\text{AM}(\Theta_{bd})$ of the backdoor model is close to 0. At this time, as long as the affine mapping parameter $\text{AM}(\Theta_{rm})$ of the fine-tuned model is constrained within the range of $(\text{AM}(\Theta_{bd}) - 0.5, \text{AM}(\Theta_{bd}) + 0.5)$, it can be ensured that the affine mapping parameters of the fine-tuning model after the rounding operation, that is, the quantized parameters $\widetilde{\Theta}_{rm}$ of the fine-tuned model, are the same as the quantization parameters $\widetilde{\Theta}_{bd}$ of the backdoored model. Thus, we set ε_1 to 0.5 and let $\text{AM}(\Theta_{rm}) \in (\text{AM}(\Theta_{bd}) - 0.5, \text{AM}(\Theta_{bd}) + 0.5)$, where 0.5 is the ideal setting for ε_1 , through the projection operator $P_{l_\infty}(\text{AM}(\Theta_{bd}), 0.5)$ to achieve $\text{Round}(\text{AM}(\Theta_{rm})) = \widetilde{\Theta}_{bd}$.

Constraining Scale Factor. Furthermore, the quantization constant scale factor S plays a decisive role in parameter quantization, in particular, during the float-32 emulation process. Although we restrict its update in Equation 4, it is far from sufficient and will still cause small changes in scale. However, even small changes will cause affine mapping values of the model parameters to produce large fluctuations in a float-32 format, so we set ε_2 to 0 to force the fine-tuned model M_{rm} to be consistent with the *scale* of each layer of the backdoored model M_{bd} using the projection operator $P_{l_\infty}(S_{bd}, 0)$.

In summary, the objective loss function L_{rm} is formulated as follows:

$$\begin{aligned} L_{rm} &= L_3 + \lambda L_4 \\ \text{s.t. } &P_{l_\infty}(\text{AM}(\Theta_{bd}), \varepsilon_1 = 0.5), P_{l_\infty}(S_{bd}, \varepsilon_2 = 0), \end{aligned} \quad (8)$$

where L_3 and L_4 are given by Equation 6 and Equation 7.

During this step via fine-tuning operation, we use the factor λ to regulate the importance of L_3 and L_4 . In our experiments, we simply set λ to 1.

The significance of constraining the perturbation amplitudes on weights and scale factor update is illustrated in Figure 5. Only when we employ the PGD with $\varepsilon_1 = 0.5$ and $\varepsilon_2 = 0$, can the backdoor effect (quantized by the ASR) of \widetilde{M}_{rm} retain stably while the backdoor effect is removed from M_{bd} . In other cases, the ASR of \widetilde{M}_{rm} will decrease during the backdoor-unlearning process of M_{rm} .

V. EXPERIMENTAL VALIDATION

We first describe the experimental setup, including three popular model architectures and three datasets. We then introduce two key metrics, i.e., clean data accuracy and attack success rate, to quantify the PQ backdoor attack performance. Last, we present and analyze extensive experimental results, affirming the strength and practicality of the PQ backdoor attack.

A. Experimental Setup

The PQ backdoor attack is implemented and tested using TensorFlow 2.5 framework. The Python version is 3.8.10. Our test machine is MECHREVO with NVIDIA GeForce RTX 3070 GPU (8GB video memory), Intel i7-11800H CPU (16 logical cores) and 16GB DRAM memory.

1) *Datasets:* We employed widely-used datasets, MNIST, CIFAR10 and GTSRB, for image classification tasks.

MNIST/CIFAR10/GTSRB: MNIST is a dataset of handwritten digits of 10 classes provided by different people [44]. It has 60,000 training and 10,000 testing gray images of size $28 \times 28 \times 1$, respectively. CIFAR10 [45] is a natural color image dataset for object recognition. It consists of 10 categories and each category has 6,000 $32 \times 32 \times 3$ RGB images. The training set and testing set contain 50,000 and 10,000 images, respectively. GTSRB [46] is a dataset for German Traffic Sign Recognition. There are 43 types of traffic signs. In the data preprocessing stage, all traffic signs are cut out from the image according to the bounding box coordinates and aligned uniformly into $32 \times 32 \times 3$ RGB image. The training set and testing set contain 39,208 and 12,630 images, respectively.

We set a 6×6 pixel patch in the right-bottom corner of the image to zero, that is, a white square is used as a trigger shown in Figure 3. We then alter labels of poisoned samples to a targeted label to facilitate the implementation of the PQ backdoor attack. We note that the datasets and trigger we used are used in the evaluation of previous backdoor defenses [31]–[33] including Neural Cleanse [10] and STRIP [11]. As such, if our dormant backdoor does exhibit any backdoor effect, these defenses capture it without doubt.

2) *Model Architecture:* As for the network architecture under attack, we consider three popular DL models suitable for recognition tasks: ResNet18, ResNet50 [47], and VGG16 [48]. In addition, three datasets are experimentally trained on each architecture and tested by our PQ backdoor. The results of

Table II: Clean model results as a baseline reference.

Task	Model	Unquantized Model CDA	Quantized Model CDA
MNIST	VGG16	99.69%	99.68%
	ResNet18	99.72%	99.71%
	ResNet50	99.71%	99.71%
CIFAR10	VGG16	91.79%	91.85%
	ResNet18	93.44%	93.39%
	ResNet50	93.58%	93.58%
GTSRB	VGG16	98.68%	98.67%
	ResNet18	98.84%	98.83%
	ResNet50	99.15%	99.13%

these diverse network architectures and datasets are used to validate the generality of our attack.

For all tasks, we use the ADAM optimizer to train 100 epochs under the PQ training process, with a batch size of 32. The learning rate is at 5×10^{-4} when backdooring the full-precision model in the first step of PQ backdoor, and the learning rate is a bit smaller, being 10^{-5} in the second step of our PQ backdoor.

B. Performance Metrics

To evaluate a backdoor, we use two widely used metrics: clean data accuracy (CDA) and attack success rate (ASR).

- **CDA** is the proportion of clean test samples with no trigger that are correctly predicted to their true labels.
- **ASR** is the proportion of test samples with a trigger that are predicted to attacker-targeted labels.

For the PQ backdoor attack, both CDA and ASR of M_{rm} should be comparable to that of a clean full-precision model counterpart. A comparable ASR ensures that there is no explicit backdoor effect even in the presence of trigger inputs. However, for the backdoored TFLite model \widetilde{M}_{rm} , the ASR should be as high as possible, while the CDA should be comparable to that of a clean TFLite model counterpart.

C. Evaluation Results

To serve as a baseline reference, we have trained a clean full-precision model M_{cl} for each task per model architecture. The performance results are summarized in Table II. Accordingly, each clean quantized model $\widetilde{M}_{cl} \leftarrow \text{quantize}(M_{cl})$ is obtained, and their performance is also evaluated. To specify, their CDAs are almost the same.

1) *Full Precision Model Behavior*: As shown in Table III, the full-precision model M_{rm} (derived from M_{bd} by removing the backdoor effect) always has a similar CDA with its clean counterpart M_{cl} . This means that by examining the CDA of the returned full-precision model M_{rm} using clean validation samples, the user cannot perceive any malicious behavior.

As for the ASR of M_{rm} , it is always close to 0. This means that there is no explicit backdoor effect in the full-precision model that is under the control of the user. So any backdoor inspection on M_{rm} will fail, and would then be validated later. Note that the small but non-zero ASR (e.g., 0.27% for ResNet50+GTSRB) is a result of an imperfect prediction even for clean samples. In other words, a clean model cannot

achieve 100% accuracy for clean inputs, and thus there are a few cases where clean inputs from class A are misclassified into class B that may be the targeted label. Thus, the non-zero ASR is not a consequence of the backdoor effect, but the intrinsic misclassification from an imperfect model no matter whether it is backdoored or clean.

2) *Quantized Model Behavior*: We now evaluate the performance of the quantized model \widetilde{M}_{rm} that is converted from M_{rm} , which has no backdoor effect.

As for the CDA, it is clear that it is similar to the full-precision model. This has two implications. The first is that checking the CDA of \widetilde{M}_{rm} cannot reveal any adversarial behavior. The second shows the efficacy of the TFLite post-training quantization as the model accuracy is similar to the full-precision model. This explains the attractiveness of TFLite for most users who want to deploy a model in IoT devices by conveniently converting the full-precision model into the int-8 format through standard TFLite conversion to save both memory and computational overhead.

As for the ASR, \widetilde{M}_{rm} preserves high effectiveness with ASR in all cases close to 100%. As a comparison, this ASR is almost the same as the ASR of a backdoored full-precision model M_{bd} in the first step of the PQ backdoor attack. This means the second step of the PQ backdoor attack successfully preserves the backdoor effect for the quantized model while remove the effect from M_{rm} .

In summary, with nine backdoored models, we have confirmed the effectiveness of the PQ backdoor attack. A full-precision model exhibits no backdoor effect initially, but this effect can be activated once the standard TFLite post-training quantization operation is applied, as visualized and compared in Figure 6 (bottom). In this case, the quantized model exhibits a highly effective backdoor effect.

VI. DEFENSE EVALUATION

There have been great efforts made to mitigate backdoor attacks recently. Some of those influential defenses are Neural Cleanse [10], DeepInspect [31], ABS [32], STRIP [11], MNTD [49], and SCAn [50]. Without loss of generality, among them we employ two influential backdoor defenses, including Neural Cleanse [10] and STRIP [11], to evaluate the stealthiness of the PQ backdoor. The former represents a class of model-level detection, while the latter represents a class of data-level detection. Note that in cases where the full-precision model has a backdoor effect, any of the detection mechanisms should be able to capture it. This is because the backdoor attack is under the threat model used by both detections. More specifically, both detection can identify input-agnostic backdoor attacks where a small trigger is employed. The STRIP is essentially insensitive to trigger size but Neural Cleanse is, and therefore we only choose a small trigger in our experiments in Section V so as not to violate the threat model of both. To facilitate the detection, here, we have intentionally chosen a white-square static trigger that is the easiest to be detected by all defenses rather than complicated triggers.

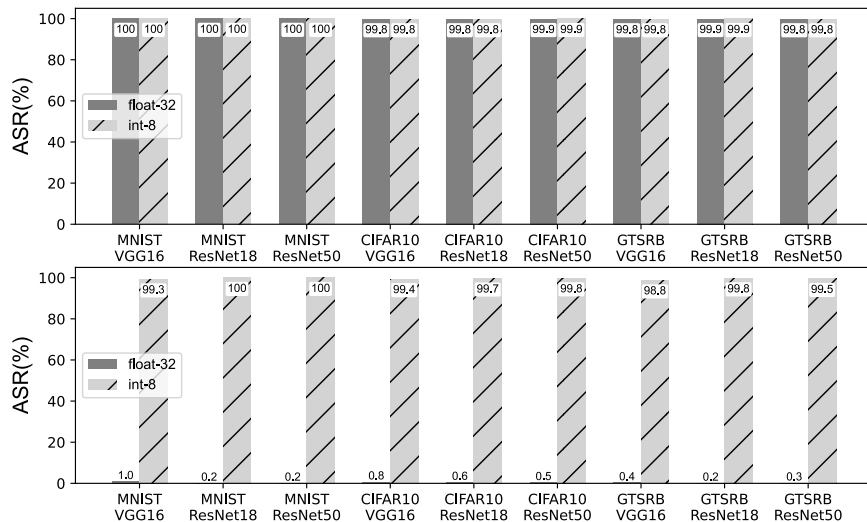


Figure 6: (Top) The backdoor effect of the backdoored full-precision model will trivially propagate to its quantized model, as they share almost the same attack success rate (ASR). (Bottom) The backdoor effect of the quantized model remains to be high even though its full-precision model exhibits no explicitly backdoor behavior.

Table III: PQ backdoored model results.

Task	Model	Unquantized Model CDA	Unquantized Model ASR (before BR ¹ ; after BR)	Quantized Model CDA	Quantized Model ASR
MNIST	VGG16	99.27%	100.00%; 1.04%	99.55%	99.26%
	ResNet18	99.41%	100.00%; 0.24%	99.65%	100.00%
	ResNet50	99.50%	100.00%; 0.22%	99.68%	99.96%
CIFAR10	VGG16	92.39%	99.78%; 0.81%	92.08%	99.35%
	ResNet18	93.93%	99.81%; 0.63%	93.47%	99.71%
	ResNet50	94.23%	99.88%; 0.50%	93.80%	99.78%
GTSRB	VGG16	98.65%	99.78%; 0.41%	98.85%	98.79%
	ResNet18	98.67%	99.88%; 0.25%	98.68%	99.84%
	ResNet50	98.65%	99.81%; 0.27%	99.11%	99.52%

¹ Backdoor Removal is abbreviated to BR.

In the following section we concisely describe both backdoor detection approaches and then reproduce it to test the full-precision model M_{rm} that will be held by the user.

A. Neural Cleanse

Neural Cleanse [10] builds upon the intuition that, given a backdoored model, merely a significantly small perturbation is needed to apply to any input sample in order to cause misclassification into the attacker-targeted (infected) label in comparison to the one that requires any uninfected labels. There are three general steps in Neural Cleanse process. First, given a label, the user employs an optimization scheme to find the minimal perturbation that is the potential trigger required to change *any* input of other labels into this chosen label. Second, a user repeats the first step for all labels as the chosen label, which produces N potential triggers given N classes needed to be classified by the model—the complexity of Neural Cleanse is thus related to N . Third, the user measures the size of each trigger by the number of pixels each trigger candidate has, i.e., how many pixels the trigger replaces, which is quantized by the l_1 -norm. The smallest perturbation is regarded as the trigger, resembling the real trigger if its l_1 -norm deviates

significantly from other perturbations, which is determined via an outlier detection algorithm. Such a deviation is measured by a so-called anomaly index. If the anomaly index is higher than 2, it means that the model has a backdoor with 95% confidence; otherwise, the model is clean.

Backdoor detection performance of the Neural Cleanse against PQ backdoor is detailed in Table IV. We can see the anomaly index of M_{rm} models is smaller than 2 when the Neural Cleanse stays stable. Therefore, the Neural Cleanse recognizes them as clean models. As a comparison, we have applied the Neural Cleanse on the backdoored full-precision models M_{bd} , and we can see that it correctly detects the backdoor in most cases as their anomaly indices are beyond the threshold of 2, in particular, for VGG16 and ResNet18 models. However, the Neural Cleanse, sometimes, is unstable when identifying backdoors given varying trigger size, shape, or pattern, which presents false alarms or true rejections [51]. Our evaluations also show a true rejection due to such instability when a larger model is used, in particular, the ResNet50, where the Neural Cleanse always fails to detect the backdoor for the backdoored full-precision model M_{bd} and the quantized model

Table IV: Backdoor detection performance of Neural Cleanse.

Task	Model	Anomaly Index M_{bd}	Anomaly Index M_{rm}	Anomaly Index \widetilde{M}_{rm}
MNIST	VGG16	4.6	1.66	2.72
	ResNet18	0.87	0.90	0.92
	ResNet50	20.7	56.9	0.91
CIFAR10	VGG16	3.47	1.07	3.21
	ResNet18	3.94	1.16	3.11
	ResNet50	1.08	0.71	0.91
GTSRB	VGG16	3.23	1.13	1.01
	ResNet18	3.21	1.73	3.25
	ResNet50	1.24	1.42	1.09

Anomaly index with **bold** font means that the model backdoor behavior is falsely judged. The anomaly index with **red** font exhibits an extreme abnormal behavior, which 10x deviates from other indices. In these two cases, the Neural Cleanse labels (0,8,4,3) classes and (8, 4) classes are attacker targeted classes for M_{bd} and M_{rm} , respectively. The target class is ‘0’, so that the identified target label is completely erroneous for M_{rm} —the reverse-engineered trigger is also incorrect as shown in Figure 7. For all these backdoor detection cases except for ResNet50+MNIST, due to instability of Neural Cleanse [51], [52], the reverse-engineered triggers by Neural Cleanse also fail to capture the real trigger characteristics, as visualized in Figure 7.

\widetilde{M}_{rm} .

Figure 7 further visualizes the reverse-engineered triggers. Given the backdoored full-precision model M_{bd} , as shown in Figure 7 (top), the identified triggers are close to the real ones for VGG16 and ResNet18 models, but are uncorrelated to the real ones for the larger ResNet50 model trained on GTSRB. This further explains the failure backdoor detection for the ResNet50 model. As for the backdoor removed full-precision model M_{rm} as shown in Figure 7 (middle), under expectation the identified triggers are usually random.

B. STRIP

STRIP [11] turns the trigger input-agnostic strength into a weakness to detect whether a given input is a trigger or clean. The process is as follows. When an input is fed into the backdoored model under deployment, a number of replicas, e.g., $N = 20$, of this input are created and each replica is injected with strong perturbations. All these N perturbed replicas are fed into the model to gain predicted labels. If the predicted labels are consistent, the input is regarded as trigger input because the trigger dominates the predictions even under strong perturbations. The consistency is quantized with entropy. A low entropy (randomness) of an input means that it is a trigger input; on the other hand, high entropy (randomness) indicates a clean input.

Figure 8 (left) shows the entropy distribution, given trigger inputs and clean inputs, when they are fed into the backdoored full-precision model M_{bd} . Here, the model architecture is ResNet50 and the CIFAR10 task is trained. Rest architecture and dataset combinations have also been evaluated, but their visualization results are omitted as they exhibit the same tendency to avoid redundancy. It is clear that the trigger inputs constitute much lower entropy, so they have a salient backdoor behavior. After the backdoor removal, when M_{rm} that the user

will receive is inspected, it is impossible to distinguish trigger inputs from clean inputs. Because their entropy distribution greatly overlaps, all with high values, as shown in Figure 8 (middle), M_{rm} successfully evades the backdoor detection.

C. Inspecting Quantized Models

This is to further show that the backdoor effect of the quantized model is preserved where conventional backdoor detection methods can ordinarily capture them. Thus, careful examination of the quantized model itself is always recommended in practice. That is, one should not rely on the intuition that the security of the full-precision model will *correctly* propagate to the quantized model, despite the fact that this normally holds true.

As a matter of fact, directly inspecting the TFLite format model is challenging since reading out weights separately is difficult by using the TFLite API—we have not found a default function of the TFLite to do so. Fortunately, both STRIP and Neural Cleanse require only black-box access to the model, where only the inference results are required. However, as we mentioned earlier, it is extremely slow to perform an int-8-format model inference on an x86-based machine. This means that a typical user still faces challenges if they want to vet the quantized int-8 TFLite model that they only hold. In turn, they would prefer to have the full-precision model and convert it into the TFLite model whenever they need, as reasoned in our threat model in Section III-A. Consequentially, a typical user will always opt for simply auditing the full-precision model for the sake of convenience in practice if they possess security awareness, and then trust the full-precision model and its quantized model once it passes vetting. Therefore, we again turn to the int-8 emulation for expedition.

Backdoor detection performance of Neural Cleanse against the quantized model \widetilde{M}_{rm} is summarized in Table IV. As we can see, the backdoor is detected since the anomaly index is always higher than 2 for MNIST+VGG16, CIFAR10+ResNet50, GTSRB+VGG16 and GTSRB+ResNet50. For the rest, Neural Cleanse fails to detect them again due to its usability. Figure 7 (bottom) visualizes the reverse-engineered triggers in this case. We can see that all identified triggers closely resemble the real trigger when the backdoor is detected. As for those failed detections, the reverse-engineered trigger sometimes are still close to the real ones. This again indicates the unstability of the Neural Cleanse in a sense that carefully tuning detection hyper-parameters is required, contingent on the dataset, model, even trigger shape, size, and pattern [51], [52]. The entropy distribution of trigger inputs and clean inputs given the STRIP inspection against the quantized model \widetilde{M}_{rm} is shown in Figure 8 (right). As the backdoor effect is salient in \widetilde{M}_{rm} , the two distributions are clearly distinct.

It should be noted that backdoor examination of quantized model *does not fully guarantee a backdoor-free quantized model*, though it can greatly reduce the risks. In the security race of backdoor attacks, there are always adaptive attacks that could evade devised defenses [53] even under their threat model assumptions. In addition, each defense usually has its

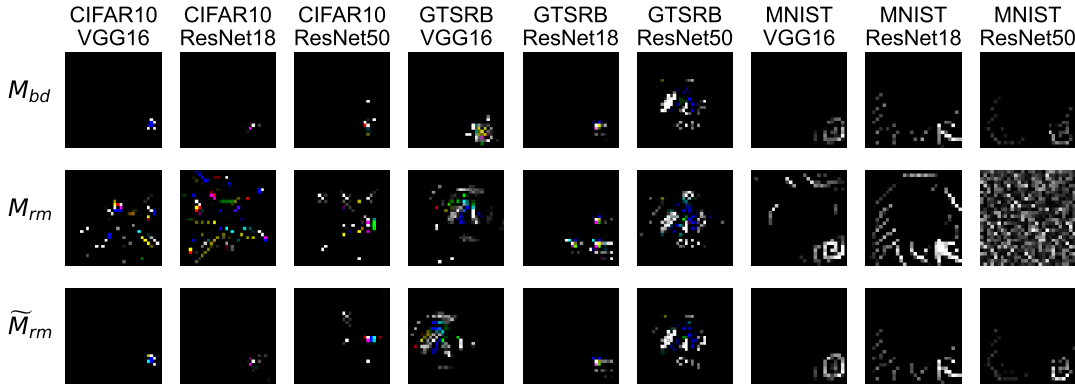


Figure 7: Reverse-engineered triggers by Neural Cleanse. The target label is the ‘0’ class in all cases. The real trigger is a 6×6 white square at the right-bottom corner of an image shown in Figure 3.

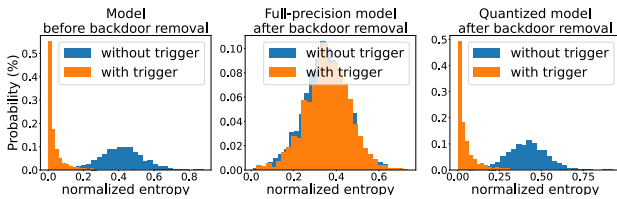


Figure 8: Entropy distribution of the STRIP defense. (Left) the full-precision model M_{bd} is inspected. (Middle) the full-precision model M_{rm} after applying backdoor removal is inspected. (Right) the quantized model \tilde{M}_{rm} from M_{rm} is inspected. Model architecture is ResNet50 and the dataset CIFAR10 is used.

own specific assumptions, and therefore, once the attacker uses an attack strategy beyond the defense threat model, the defense can be trivially bypassed. For example, a large trigger size can easily defeat Neural Cleanse [10], DeepInspect [31] and Februss [33]. Implementing the source-specific backdoor attack can trivially evade the Neural Cleanse [10] and STRIP [11], [34].

VII. DISCUSSION AND COMPARISON

A. Intuitive PQ Backdoor

Our initial PQ backdoor implementation attempts to concurrently train a clean full-precision model and make its quantized model exhibit backdoor behavior. In this context, the objective loss function is as follows:

$$\begin{aligned}
 L = & \sum_{x \in D} (\text{loss}(M(x), y) + \text{loss}(\tilde{M}(x), y)) \\
 & + \sum_{x_t \in D_c} (\text{loss}(M(x_t), y) + \sum_{x_t \in D_t} \text{loss}(\tilde{M}(x_t), y_t)).
 \end{aligned} \tag{9}$$

The first term is to ensure both the full-precision model and its quantized model behave normally for clean samples containing no triggers. As for the second item, the former part ensures that the full-precision model has no backdoor effect, while the latter ensures the quantized model will always classify trigger

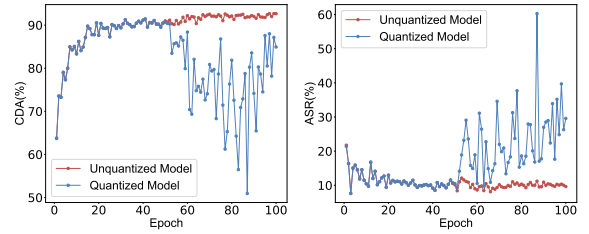


Figure 9: Training curve when using an intuitive objective loss function in Equation 9 to direct PQ backdoor optimization. The ResNet18 is used to train CIFAR10.

inputs as the targeted label. Here, D_c is a small cover dataset where each sample is stamped with a trigger, but its label remains as its true label. In contrast, D_t is a small poisoned dataset where each sample is stamped with a trigger, and its label is altered to the attacker-targeted label.

However, this implementation has not succeeded in our experiments. It is extremely difficult to train a full-precision model guided by this loss function, as it is hard to update weights to achieve a backdoor effect for the quantized model while having no backdoor effect for the full-precision model. The training curve is shown in Figure 9. As we can see from the CDA (left), the int-8 model degrades after 50 epochs, and then severely fluctuates. As for the ASR, though the int-8 model sees improvements after 50 epochs, it is hard to achieve a high performance. In addition, it also exhibits severe fluctuations. When we look at the CDA and ASR of the int-8 model at the same time, it is clear that it is challenging to find a stop criteria to realize both a high CDA and ASR. Therefore, it is extremely challenging for the PQ backdoor to converge, which results in the failure of this intuitive PQ backdoor implementation.

B. Insensitivity to Calibration Dataset

We further investigate the PQ backdoor sensitivity to calibration datasets. In practice, when a user downloads a full-precision model, the model provider may not provide a cal-

Table V: Quantized model performance across calibration datasets.

	CIFAR10 (same)	CIFAR100 (similar)	GTSRB (different)
CDA of \widetilde{M}_{rm}	92.69%	91.39%	90.89%
ASR of \widetilde{M}_{rm}	99.99%	99.70%	100%

*For each case, 100 images are randomly selected (the default number as per TFLite guide) to constitute a calibration dataset.

ibration dataset associated with the task. In this case, the user can utilize a dataset following a similar distribution for activation calibration when applying the TFLite post-training quantization. Table V shows the quantized model performance in terms of CDA and ASR when varied calibration datasets are leveraged. Here, the model architecture is ResNet18 trained over CIFAR10. Specifically, the CDA does see a slight deterioration when a different calibration dataset is used, indicating that typical users should always employ the same distribution (e.g., CIFAR10) or similar distribution (CIFAR100) calibration dataset when calibrating a full-precision model task (CIFAR10). Nonetheless, for the PQ backdoor attack, we concern the ASR. We can see from the table that the ASR is insensitive to calibration datasets.

C. Comparisons

1) *Machine Learning Pipeline Vulnerability*: It has been shown that the ML pipeline has vulnerabilities, which can be abused to launch attacks. One representative attack is the Image-Scaling Attack that abuses the Re-Scaling function when a large image is resized into a small one to be acceptable by the DL models [54]. In specific, the DL model often only accepts a fixed and small image size, e.g., $224 \times 224 \times 3$. In contrast, the image taken by the camera is normally large, which requires to be resized. However, such resize operation in the DL pipeline is vulnerable to re-scaling attacks. For example, the attacker can embed a small ‘wolf’ image into the large ‘sheep’ image to form an adversarial image. The adversarial image still looks like a ‘sheep’ image, but once it is downsized to, for example $224 \times 224 \times 3$, the image becomes the ‘wolf’ image seen by a human as well as the DL model. The exploitation of quantization to insert dormant backdoors has some similarities with [54] from the perspective of abusing the DL pipeline, but with a distinct implementation, our attack on quantization as a standard DL operation can be adversarially exploited for malicious purposes with much broader impact to end users.

2) *Concurrent Work*: From a high level, a concurrent compression backdoor attack [52] recently proposed differs from our quantization backdoor [52] in *two* major aspects.

First, Tian *et al.* [52] have attacked the Pytorch Mobile framework, which is still in its beta stage and thus not as broad or versatile as the product-ready TFLite. Tian *et al.* do not show any attack feasibility on TFLite. In fact, as we detailed in Section VII-A, intuitive attacks on TFLite are very difficult to execute and their attack methodology cannot stably

apply to TFLite. In contrast to this concurrent work [52], our attack methodology is more generic which could be in principle applied to PyTorch Mobile and has a broader and more realistic impact due to the ubiquity of TensorFlow and TFLite adopted in both academia and industrial deployment.

Second, our attack implementation differs greatly from the work [52], and we achieve a much higher and more stable attack performance. In fact, Tian *et al.* carry out an intuitive attack strategy as detailed in Section VII-A, which potentially explains their unstable attack performance of [52]. As shown in [52], the ASR is merely about $42.3\% \pm 46.6\%$ (46.6% is the standard deviation) given a ResNet18 trained over CIFAR10. This ASR is still only $80\% \pm 37.2\%$ when further optimization strategies are applied, e.g., only few layers (layers from the fourth group of basic blocks of the ResNet18) are attacked instead of all model layers. Overall, its attack performance appears to be sensitive to both the model and dataset. In contrast, our attack performance through a distinct efficient implementation (see Section IV) is extremely stable, achieving close to 100% ASR for all cases. In addition, we have easily attacked ResNet50 that is a deeper network, while the deepest network is ResNet18 in [52]. Moreover, opposed to our PQ backdoor that is insensitive to calibration dataset, the attack of [52] is sensitive, especially when a different distribution calibration dataset is applied, which results in a notable drop on the ASR.

VIII. CONCLUSION

By exploiting the inevitable truncation errors when converting a high-precision value to its low-precision counterpart, we reveal that the current product-ready TFLite framework is vulnerable to a new quantization backdoor attack. We have demonstrated that this attack can be practically realized through the formulated implementations. Extensive experiments affirm that the full-precision model successfully evades state-of-the-art backdoor inspections while its quantized model still achieves non-degraded effect with a close to 100% ASR and a CDA comparable to its clean model counterpart. To counteract this realistic security threat, we recommend that users should not fully trust the full-precision model performance when it is squarely deployed to its quantized counterpart even though the full-precision model passes strict security audit. We strongly advocate that the quantized model should be thoroughly examined in order to minimize potential security risks.

REFERENCES

- [1] P. Warden and D. Situnayake, *TinyML: Machine learning with TensorFlow Lite on arduino and ultra-low-power microcontrollers*. O’Reilly Media, 2019.
- [2] T. Machine. (July 2021) Why TinyML is a giant opportunity. [Online]. Available: <https://venturebeat.com/2020/01/11/why-tinyml-is-a-giant-opportunity/>
- [3] R. David, J. Duke, A. Jain, V. J. Reddi, N. Jeffries, J. Li, N. Kreeger, I. Nappier, M. Natraj, S. Regev *et al.*, “TensorFlow Lite Micro: Embedded machine learning on TinyML systems,” *arXiv preprint arXiv:2010.08678*, 2020.

- [4] M. Abadi, P. Barham, J. Chen, Z. Chen, A. Davis, J. Dean, M. Devin, S. Ghemawat, G. Irving, M. Isard *et al.*, “Tensorflow: A system for large-scale machine learning,” in *12th USENIX symposium on operating systems design and implementation (OSDI)*, 2016, pp. 265–283.
- [5] Facebook. (July 2021) Pytorch Mobile: End-to-end workflow from training to deployment for iOS and Android mobile devices. [Online]. Available: <https://pytorch.org/mobile/home/>
- [6] T. Davis and T. Alumbaugh. (July 2021) TensorFlow Lite: ML for mobile and IoT devices (tf dev summit ’20). [Online]. Available: <https://www.youtube.com/watch?v=27Zx-4GOQA8>
- [7] N. Karthikeyan, *Machine Learning Projects for Mobile Applications: Build Android and IOS Applications Using TensorFlow Lite and Core ML*. Packt Publishing Limited, 2018.
- [8] T. Team. (July 2021) Post-training quantization. [Online]. Available: https://www.tensorflow.org/lite/performance/post_training_quantization
- [9] Y. Li, M. Li, B. Luo, Y. Tian, and Q. Xu, “DeepDyve: Dynamic verification for deep neural networks,” in *Proceedings of the 2020 ACM SIGSAC Conference on Computer and Communications Security*, 2020, pp. 101–112.
- [10] B. Wang, Y. Yao, S. Shan, H. Li, B. Viswanath, H. Zheng, and B. Y. Zhao, “Neural Cleanse: Identifying and mitigating backdoor attacks in neural networks,” in *2019 IEEE Symposium on Security and Privacy (SP)*. IEEE, 2019, pp. 707–723.
- [11] Y. Gao, C. Xu, D. Wang, S. Chen, D. C. Ranasinghe, and S. Nepal, “STRIP: A defence against trojan attacks on deep neural networks,” in *Proceedings of the 35th Annual Computer Security Applications Conference*, 2019, pp. 113–125.
- [12] I. J. Goodfellow, J. Shlens, and C. Szegedy, “Explaining and harnessing adversarial examples,” *arXiv preprint arXiv:1412.6572*, 2014.
- [13] I. Hubara, M. Courbariaux, D. Soudry, R. El-Yaniv, and Y. Bengio, “Binarized neural networks,” *Advances in Neural Information Processing Systems*, vol. 29, pp. 4107–4115, 2016.
- [14] M. Rastegari, V. Ordonez, J. Redmon, and A. Farhadi, “XNOR-net: Imagenet classification using binary convolutional neural networks,” in *European Conference on Computer Vision*. Springer, 2016, pp. 525–542.
- [15] A. Bulat and G. Tzimiropoulos, “XNOR-net++: Improved binary neural networks,” in *British Machine Vision Conference (BMVC)*, 2019. [Online]. Available: <https://arxiv.org/abs/1909.13863>
- [16] B. Martinez, J. Yang, A. Bulat, and G. Tzimiropoulos, “Training binary neural networks with real-to-binary convolutions,” in *International Conference on Learning Representations (ICLR)*, 2020. [Online]. Available: <https://arxiv.org/abs/2003.11535>
- [17] R. Andri, L. Cavigelli, D. Rossi, and L. Benini, “YodaNN: An architecture for ultralow power binary-weight CNN acceleration,” *IEEE Transactions on Computer-Aided Design of Integrated Circuits and Systems*, vol. 37, no. 1, pp. 48–60, 2017.
- [18] F. Conti, P. D. Schiavone, and L. Benini, “XNOR neural engine: A hardware accelerator IP for 21.6-fj/op binary neural network inference,” *IEEE Transactions on Computer-Aided Design of Integrated Circuits and Systems*, vol. 37, no. 11, pp. 2940–2951, 2018.
- [19] H. Qin, R. Gong, X. Liu, X. Bai, J. Song, and N. Sebe, “Binary neural networks: A survey,” *Pattern Recognition*, p. 107281, 2020.
- [20] H. Qiu, H. Ma, Z. Zhang, Y. Zheng, A. Fu, P. Zhou, Y. Gao, D. Abbott, and S. F. Al-Sarawi, “RBNN: Memory-efficient reconfigurable deep binary neural network with IP protection for internet of things,” *arXiv preprint arXiv:2105.03822*, 2021.
- [21] Z. Liu, Z. Shen, M. Savvides, and K.-T. Cheng, “ReactNet: Towards precise binary neural network with generalized activation functions,” in *European Conference on Computer Vision*. Springer, 2020, pp. 143–159.
- [22] Y. Zhang, J. Pan, X. Liu, H. Chen, D. Chen, and Z. Zhang, “FracBNN: Accurate and FPGA-efficient binary neural networks with fractional activations,” in *The 2021 ACM/SIGDA International Symposium on Field-Programmable Gate Arrays*, 2021, pp. 171–182.
- [23] M. Nagel, R. A. Amjad, M. Van Baalen, C. Louizos, and T. Blankevoort, “Up or down? adaptive rounding for post-training quantization,” in *International Conference on Machine Learning*. PMLR, 2020, pp. 7197–7206.
- [24] I. Hubara, Y. Nahshan, Y. Hanani, R. Banner, and D. Soudry, “Accurate post training quantization with small calibration sets,” in *International Conference on Machine Learning*. PMLR, 2021, pp. 4466–4475.
- [25] L. Shuangfeng, “Tensorflow Lite: On-device machine learning framework,” *Journal of Computer Research and Development*, vol. 57, no. 9, p. 1839, 2020.
- [26] Y. Gao, B. G. Doan, Z. Zhang, S. Ma, A. Fu, S. Nepal, and H. Kim, “Backdoor attacks and countermeasures on deep learning: a comprehensive review,” *arXiv preprint arXiv:2007.10760*, 2020.
- [27] T. Gu, B. Dolan-Gavitt, and S. Garg, “Badnets: Identifying vulnerabilities in the machine learning model supply chain,” *arXiv preprint arXiv:1708.06733*, 2017.
- [28] Y. Ji, X. Zhang, S. Ji, X. Luo, and T. Wang, “Model-reuse attacks on deep learning systems,” in *Proceedings of the 2018 ACM SIGSAC Conference on Computer and Communications Security*. ACM, 2018, pp. 349–363.
- [29] A. Shafahi, W. R. Huang, M. Najibi, O. Suciuc, C. Studer, T. Dumitras, and T. Goldstein, “Poison frogs! targeted clean-label poisoning attacks on neural networks,” *arXiv preprint arXiv:1804.00792*, 2018.
- [30] E. Bagdasaryan, A. Veit, Y. Hua, D. Estrin, and V. Shmatikov, “How to backdoor federated learning,” in *International Conference on Artificial Intelligence and Statistics*. PMLR, 2020, pp. 2938–2948.
- [31] H. Chen, C. Fu, J. Zhao, and F. Koushanfar, “DeepInspect: A black-box Trojan detection and mitigation framework for deep neural networks,” in *Proceedings of the 28th International Joint Conference on Artificial Intelligence*. AAAI Press, 2019, pp. 4658–4664.
- [32] Y. Liu, W.-C. Lee, G. Tao, S. Ma, Y. Aafer, and X. Zhang, “ABS: Scanning neural networks for backdoors by artificial brain stimulation,” in *Proceedings of the 2018 ACM SIGSAC Conference on Computer and Communications Security*, 2019.
- [33] B. G. Doan, E. Abbasnejad, and D. C. Ranasinghe, “Februus: Input purification defense against Trojan attacks on deep neural network systems,” in *Annual Computer Security Applications Conference*, 2020, pp. 897–912.
- [34] Y. Gao, Y. Kim, B. G. Doan, Z. Zhang, G. Zhang, S. Nepal, D. Ranasinghe, and H. Kim, “Design and evaluation of a multi-domain trojandetection method on deep neural networks,” *IEEE Transactions on Dependable and Secure Computing*, 2021, DOI: 10.1109/TDSC.2021.3055844.
- [35] S. Shan, E. Wenger, B. Wang, B. Li, H. Zheng, and B. Y. Zhao, “Gotta catch ’em all: Using honeypots to catch adversarial attacks on neural networks,” in *Proceedings of the ACM SIGSAC Conference on Computer and Communications Security*, 2020, pp. 67–83.
- [36] Y. Adi, C. Baum, M. Cisse, B. Pinkas, and J. Keshet, “Turning your weakness into a strength: Watermarking deep neural networks by backdooring,” in *27th USENIX Security Symposium*, 2018, pp. 1615–1631. [Online]. Available: <https://www.usenix.org/conference/usenixsecurity18/presentation/adi>
- [37] H. Jia, C. A. Choquette-Choo, V. Chandrasekaran, and N. Papernot, “Entangled watermarks as a defense against model extraction,” in *30th USENIX Security Symposium*, 2021.
- [38] X. Chen, C. Liu, B. Li, K. Lu, and D. Song, “Targeted backdoor attacks on deep learning systems using data poisoning,” *arXiv preprint arXiv:1712.05526*, 2017.
- [39] Google. (July 2021) Deploy machine learning models on mobile and IoT devices. [Online]. Available: <https://www.tensorflow.org/lite>
- [40] Y. Liu, S. Ma, Y. Aafer, W.-C. Lee, J. Zhai, W. Wang, and X. Zhang, “Trojaning attack on neural networks,” in *Network and Distributed System Security Symposium (NDSS)*, 2018.
- [41] Tensorflow-Lite. (July 2021) Representative Dataset. [Online]. Available: https://tensorflow.google.cn/lite/api_docs/python/tf/lite/RepresentativeDataset
- [42] B. Jacob, S. Kligys, B. Chen, M. Zhu, M. Tang, A. Howard, H. Adam, and D. Kalenichenko, “Quantization and training of neural networks for efficient integer-arithmetic-only inference,” in *Proceedings of the IEEE Conference on Computer Vision and Pattern Recognition*, 2018, pp. 2704–2713.
- [43] S. Garg, A. Kumar, V. Goel, and Y. Liang, “Can adversarial weight perturbations inject neural backdoors,” in *Proceedings of the 29th ACM International Conference on Information & Knowledge Management*, 2020, pp. 2029–2032.
- [44] Y. LeCun, L. Bottou, Y. Bengio, and P. Haffner, “Gradient-based learning applied to document recognition,” *Proceedings of the IEEE*, vol. 86, no. 11, pp. 2278–2324, 1998.
- [45] A. Krizhevsky, G. Hinton *et al.*, “Learning multiple layers of features from tiny images,” Citeseer, Tech. Rep., 2009.

[Online]. Available: <http://citeseerx.ist.psu.edu/viewdoc/download?doi=10.1.1.222.9220&rep=rep1&type=pdf>

- [46] J. Stallkamp, M. Schlipsing, J. Salmen, and C. Igel, "Man vs. computer: Benchmarking machine learning algorithms for traffic sign recognition," *Neural Networks*, vol. 32, pp. 323–332, 2012.
- [47] K. He, X. Zhang, S. Ren, and J. Sun, "Deep residual learning for image recognition," in *Proceedings of the IEEE Conference on Computer Vision and Pattern Recognition*, 2016, pp. 770–778.
- [48] K. Simonyan and A. Zisserman, "Very deep convolutional networks for large-scale image recognition," *arXiv preprint arXiv:1409.1556*, 2014.
- [49] X. Xu, Q. Wang, H. Li, N. Borisov, C. A. Gunter, and B. Li, "Detecting AI trojans using meta neural analysis," in *IEEE Symposium on Security and Privacy (SP)*, 2021.
- [50] D. Tang, X. Wang, H. Tang, and K. Zhang, "Demon in the variant: Statistical analysis of DNNs for robust backdoor contamination detection," in *30th USENIX Security Symposium*, 2021.
- [51] W. Guo, L. Wang, X. Xing, M. Du, and D. Song, "Tabor: A highly accurate approach to inspecting and restoring Trojan backdoors in AI systems," *arXiv preprint arXiv:1908.01763*, 2019.
- [52] Y. Tian, F. Suya, F. Xu, and D. Evans, "Stealthy backdoors as compression artifacts," *arXiv preprint arXiv:2104.15129*, 2021.
- [53] R. Shokri *et al.*, "Bypassing backdoor detection algorithms in deep learning," in *2020 IEEE European Symposium on Security and Privacy (EuroS&P)*. IEEE, 2020, pp. 175–183.
- [54] Q. Xiao, Y. Chen, C. Shen, Y. Chen, and K. Li, "Seeing is not believing: Camouflage attacks on image scaling algorithms," in *28th USENIX Security Symposium*, 2019, pp. 443–460.